

DETERMINATION OF SURFACE CHARGE DENSITY OF α -ALUMINA BY ACID - BASE TITRATION

Justin W. Ntalikwa

Department of Chemical and Process Engineering, University of Dar es Salaam, P.O. Box
35131, Dar es Salaam, Tanzania

(Received February 8, 2005; revised August 26, 2006)

ABSTRACT. The surface charge density (σ_0) of colloidal alpha alumina suspended in various 1:1 electrolytes was measured using acid-base titration. An autotitrator capable of dispensing accurately $25 \pm 0.1 \mu\text{L}$ of titrant was used. The pH and temperature in the titration cell were monitored using single junction electrodes and platinum resistance thermometers, respectively. A constant supply of nitrogen gas in the cell was used to maintain inert conditions. The whole set up was interfaced with a computer for easy data acquisition. It was observed that the material exhibits a point of zero charge (PZC), this occurred at pH of 7.8 ± 0.1 , 7.6 ± 0.2 , 8.5 ± 0.1 , 8.3 ± 0.1 for NaCl, NaNO₃, CsCl and CsNO₃ systems, respectively. It was also observed that below PZC, σ_0 increases with increase in electrolyte concentration (C_0) whereas above PZC, σ_0 decreases with increase in C_0 . It was concluded that σ_0 of this material is a function of pH and C_0 and that its polarity can be varied through zero by varying these parameters.

KEY WORDS: Alumina, Surface charge density, Acid-base titration, Point of zero charge

INTRODUCTION

Alumina is an oxide of aluminium that exists in various forms with different crystalline structures. The stable form of alumina is α -Al₂O₃ (corundum), it has rhombohedral crystalline structure and it occurs naturally in various types of rocks. The other forms of alumina (β -Al₂O₃ and γ -Al₂O₃) are unstable and they can be heated under controlled temperatures to form the stable form α -Al₂O₃ [1, 2]. Alumina exhibits both acidic and alkaline properties when dispersed in water and consequently it is classified as an amphoteric oxide [3]. Alumina has many technical applications.

In chemical and process industries, it is used in the manufacture of abrasives, paints, toothpaste, catalysts, glass, pigments and other various types of chemicals such as Al₂(SO₄)₃, AlCl₃, synthetic zeolites, etc, which have numerous applications. For instance, Al₂(SO₄)₃ is used in water purification to coagulate or flocculate suspended particles. The suspended flocs or aggregates settle at the bottom of the equipment and they can be removed as slurry, leaving essentially clear water.

In the paper industry, it is used as filler. It fills the voids between the fibres and assists smooth paper formation and increases the opacity of paper. It is also used as filler in making various rubber and plastic products. In the ceramic industry, it is used in various formulations to make different ceramic products and refractories suitable for various ranges of furnace temperatures.

Alumina has very high melting point (2045 °C), good hardness (Mohs scale 9), low volatility and is chemically inert. Due to these properties, when coupled with other materials, it is suitably used in areas that require high structural stiffness, heat resistance and low weight. These areas include manufacture of aerospace housing, automotive and jet engines and lead acid batteries [2]. In specialised industries, alumina is used in the manufacture of lightweight inorganic fibres that can be transformed into various products such as electrical insulators, filter membranes,

*Corresponding author. E-mail: jntalikwa@cpe.udsm.ac.tz

molecular sieves, thermal barriers or protectors (up to 1400 °C), seals and fibre mats. Because of these enormous applications of alumina, elucidation of its physio-chemical properties is very important.

When a mineral oxide such as alumina is dispersed in a polar medium, a cloud of oppositely charged ions normally surround its surface forming the so called an electric double layer (EDL). The interactions that occur within the EDL depend on many parameters such as the surface charge density (σ_0), surface potential (ψ_0) and nature of the surface ionisable groups adsorbed on the oxide surface. Other parameters that may affect these interactions include the concentration and composition of solutes in the dispersion medium, and the medium itself. The interactions in the EDL influence the behaviour of the mineral oxide when suspended in liquid medium. Consequently, processes such as the uptake, transport and release of adsorbed contaminants, mineral dissolution and precipitation, various redox reactions and the colloidal stability towards coagulation of the oxide dispersions depend significantly on the EDL interactions [3-6]. Thus, experimental knowledge of parameters that affect EDL interactions allows evaluation of a variety of model predictions that assist characterisation of the oxide surface.

In the present work the surface charge density (σ_0) of alumina sample suspended in various 1:1 electrolytes was measured using acid-base titration technique. The data generated herein can be used to estimate (using appropriate models) the surface potential (ψ_0) of the oxide, which is an important parameter in predicting the stability of the oxide dispersion towards coagulation.

THEORETICAL BACKGROUND

It has been established that in the presence of water, the surfaces of mineral oxides, especially those of Al, Fe and Si are generally covered with hydroxyl groups [7-10]. Surface hydration and dissociation of these groups, result into a pH dependent surface charge whose density can be measured by acid-base titration. The surface charge density determined by such method is essentially measured relative to the unknown condition of the oxide/liquid interface prior to reagent addition (i.e. at the point of zero titration). Using the acid-base titration technique, the analytical (titratable) surface charge density (σ'') at various pH values can be estimated as follows [11]:

$$\sigma'' = \frac{10^{-4} F (N_{AL} - N_{BL})}{m_p A_{sp}} \quad (1)$$

Curves of σ'' as a function of pH at various electrolyte concentrations may or may not intersect at a single point, i.e. a common intersection point (CIP). If they happen to have a CIP then the intersection point will give the titratable surface charge density at the point of zero titration (σ_s). In such situations, the surface charge density (σ_0) can be estimated from [11, 12]:

$$\sigma_0 = \sigma'' \pm \sigma_s \quad (2)$$

The knowledge of σ_0 from experimental work can allow evaluation of surface potential (ψ_0) using appropriate models such as the Gouy-Chapmann model where [11]:

$$\sigma_0 = -(8n_0 \epsilon_0 \epsilon_r kT)^{\frac{1}{2}} \sinh\left(\frac{ze\psi_0}{2kT}\right) \quad (3)$$

It can be noted that due to complex phenomena that occur at the oxide/liquid interface, there are no direct methods of measuring ψ_o . Instead, potentials at small distances (equal to the diameter of one hydrated ion) from the surface of the oxide (ψ_d) are normally measured through methods such as electrophoresis and electro-osmosis. The knowledge of ψ_o or ψ_d can enable estimation of the critical coagulation concentration (CCC) of oxide particles suspended in a liquid medium. At CCC the electric double layers formed around particle surfaces exhibit minimum repulsion and hence there are great chances of particles to bind together and form flocs. Thus, in handling slurries of oxide particles knowledge of CCC is important, as it is normally associated with change of slurry behaviour such as increase in viscosity. For spherical particles suspended in water the CCC (in mol dm⁻³) can be given as follows [11, 12]:

$$CCC = \frac{3.84 \times 10^{-39} \left(\tanh \left(\frac{ze\psi_d}{4kT} \right) \right)^4}{A^2 z^6} \quad (4)$$

EXPERIMENTAL

Materials. α -Alumina (AKP 30 grade) obtained from Mandoval Zirconia sales Ltd, UK, was used as obtained. The chemical analysis provided by the manufacturer (Table 1) suggests that the material is of very high purity.

Table 1. Chemical analysis of alumina specified by the manufacturer.

Component	Al ₂ O ₃	Fe	Si	Cu	Mg	Na
% by weight	99.99	0.002	0.005	0.001	0.001	0.001

Specific surface area. The specific surface area was determined using automated nitrogen gas adsorption and Micromeritics ASAP 2000 equipment.

Particle density. The particle density was determined by pycnometry using water as the dispersion medium.

Chemicals. All chemicals were of analytical reagent grade (obtained from Fisons Co. Ltd, Acro Organics Ltd, UK and Fisher Scientific UK). Water was produced by reverse osmosis, ion exchange, carbon adsorption and microfiltration of the local supply to pH and conductance of 5.5-5.8 and 0.7-1.2 $\mu\text{S cm}^{-1}$, respectively. Concentrated electrolytes (0.1-0.5 M) were prepared by dissolving known amount of salt in water and the dilute ones were made diluting prescribed amounts of the concentrated ones. The electrolytes were allowed to stand at least one day (24 hours) prior to use. Titrants HCl, HNO₃ and NaOH were obtained as 1.0 M standard solutions, whereas 1.0 M CsOH was made by dilution from a stock of 50 % w/w CsOH.

Sample preparation and titration. Samples were prepared by dispersing 7.3 g air dry (6.9 g oven dry) of α -alumina powder in 50 mL of electrolyte solution inside thermostatted jacketed titration cells. Samples were left to stand for 24 hours. Titrations were performed using high precision syringes (25 \pm 0.1 μL) adjusted by stepper motors (Hamilton PSD/2). Reagents were drawn into the syringes from large capacity reagent reservoirs and were delivered to samples via micro-bore tubing. Sample pH and temperature were monitored using single junction electrodes and platinum resistance thermometers, respectively. An inert atmosphere above the sample was

maintained using a supply of CO₂ free N₂. These facilities were controlled with a computer that also served as a data-logger. The system was configured to perform two titrations, essentially, in parallel. Duplicate samples were typically titrated, one with acid, the other with base, from their initial conditions at the point of zero titration (PZT).

The quantities of titrant added were adjusted using a predictor-corrector method to provide a uniform spread of experimental data points with respect to pH. Sample conditions were monitored following each addition of reagents. When sample pH was invariant with time it was assumed to be at equilibrium. Conditions were then recorded, another dose of titrant was then delivered and the process repeated until the pH reached prescribed limits. A similar procedure was used for the titration of particle free electrolytes (blank titrations). Titrations were performed in the presence of various electrolytes (NaCl, NaNO₃, CsCl and CsNO₃ in the concentration range of 0.5-10⁻⁴ M), using the conjugate acids and bases, from which they are derived, as titrants.

Data analysis. Titration data were processed to provide continuous/semi-continuous functions of pH in relation to the cumulative addition of titrant for blank and corresponding sample titrations for each electrolyte concentration. This curve fitting was adjusted to achieve a correlation coefficient (r) in the range $0.99 \leq r^2 \leq 1.00$. The functions obtained were used to calculate the corresponding cumulative titrant addition to blanks (N_{BL}) and sample (N_{AL}) at corresponding pH points. At each pH point, the value of N_{BL} was subtracted from that of N_{AL} to compensate for any reagent interaction with surfaces of the cells and facilities therein. Equation 1 was then used to provide estimates of σ'' at various pH. In circumstances where relationships obtained from titration in various concentrations of the same electrolyte possessed a common intersection point (CIP) (within an error of ± 0.2 pH units), the initial surface charge density (σ_0) at that point was determined. In such situations, the surface charge density (σ_0) was estimated using equation 2.

RESULTS AND DISCUSSION

The material was found to have a specific surface area of $7200 \pm 200 \text{ m}^2 \text{ kg}^{-1}$. The density of the material was found to be $3900 \pm 100 \text{ kg m}^{-3}$. The mean particle size on this basis is $0.40 \pm 0.01 \text{ }\mu\text{m}$ and agrees well with that determined using electrokinetic studies for a similar material [13].

NaCl and NaNO₃ systems. The effect of pH on σ'' in various concentrations of NaCl produces a family of curves which appear to have a CIP at $\text{pH} = 7.8 \pm 0.1$ and $\sigma'' = 0.8 \pm 0.1 \text{ }\mu\text{C cm}^{-2}$ (Figure 1a). This allows using equation 2 to calculate σ_0 (Figure 1b). It can be seen from Figure 1a and 1b that at pH values below the CIP the curves spread more widely than at pH below it. This observation may be explained as follows: at pH values below the CIP ($\text{pH} < 7.8$), the hydroxyl groups on the particle surface are essentially protonated resulting to a positively charged surface. However, in this region the Cl⁻ ions bind on some of the positive sites so as to create neutrality. Above the CIP ($\text{pH} > 7.8$), the hydroxyl groups on the particle surface are deprotonated resulting to a negatively charged surface and in this region Na⁺ ions bind on some of the negative sites. The spread of the curves below and above the CIP suggest that Cl⁻ ions do not bind effectively to the surface as compared to Na⁺ ions.

The CIP of NaNO₃, occurs at $\text{pH} = 7.6 \pm 0.2$ and $\sigma'' = 1.4 \pm 0.1 \text{ }\mu\text{C cm}^{-2}$ (Figure 2a). The existence of CIP in this system allows using equation 2 for estimation σ'' . The results have been presented in Figure 2b and they exhibit similar features as those of Figure 1b. From Figure 1b and 2b it can be seen that below CIP, as the electrolyte concentration increases from 10⁻⁴ to 0.5

M the values of σ_0 generally increase. However above the CIP, values of σ_0 generally decrease with increase in C_0 .

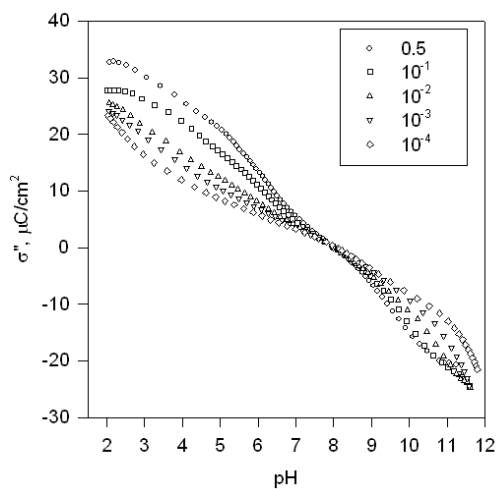


Figure 1a. Analytical surface charge density (σ'') as a function of pH in aqueous NaCl of different concentrations ($0.5-10^{-4}$ M).

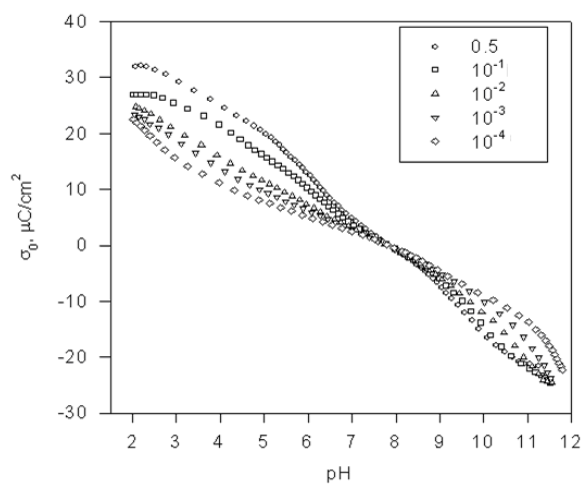


Figure 1b. Surface charge density (σ_0) as a function of pH in aqueous NaCl of different concentrations ($0.5-10^{-4}$ M).

CsCl and CsNO₃ systems. The CIP in CsCl occurs at $\text{pH} = 8.5 \pm 0.1$, $\sigma'' = -0.9 \pm 0.1 \mu\text{C cm}^{-2}$ (Figure 3a) and the estimates of σ_0 as a function of pH are presented in Figure 3b. The CIP in CsNO₃ occurs at $\text{pH} = 8.3 \pm 0.1$, $\sigma'' = -0.2 \pm 0.1 \mu\text{C cm}^{-2}$ (Figure 4a) and the corresponding estimates of σ_0 as a function of pH are shown in Figure 4b.

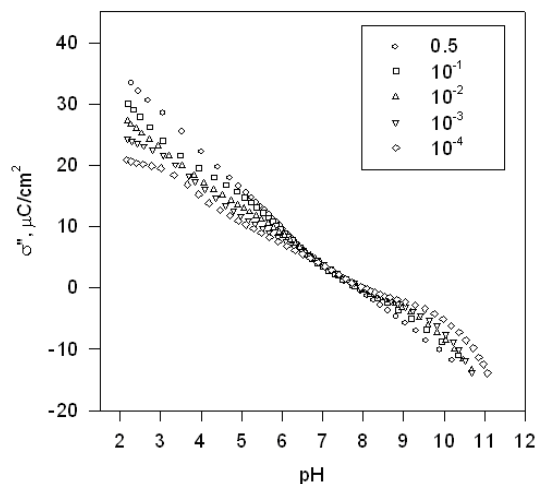


Figure 2a. σ' as a function of pH in aqueous NaNO_3 of different concentrations ($0.5\text{-}10^{-4}$ M).

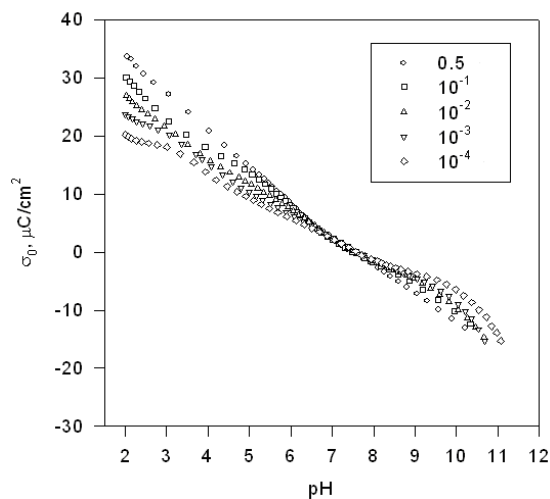


Figure 2b. σ_0 as a function of pH in aqueous of NaNO_3 of different concentrations ($0.5\text{-}10^{-4}$ M).

σ_0 as a function of the type of electrolyte. Figure 5a and 5b present the variation of σ_0 with the type of the electrolyte at constant electrolyte concentration. From these it can be seen that below CIP, CsNO_3 , NaCl and NaNO_3 appear to give same magnitudes of σ_0 whereas above the CIP, sodium salts (NaCl and NaNO_3) give low values of σ_0 compared to the cesium salts (CsCl and CsNO_3).

The trends observed in this work (Figure 1 through 5) can be explained by considering the interactions that occur at the oxide/liquid interface. It is apparent that below the CIP the positively charged surface is dominated by adsorbed anions whereas above the CIP the negatively charged surface is dominated by adsorbed cations. At $\text{pH} \leq 3$ the concentrations of anions (Cl^- and NO_3^- ions) is very high due to the addition of large quantities of HCl and HNO_3 .

in the systems investigated. Likewise, in basic conditions, ($\text{pH} \geq 10$) the concentration of cations (Na^+ and Cs^+ ions) is very high due to addition of large quantities of NaOH and CsOH . The presence of high concentrations of ions in these regions may pose a screening effect to the binding sites. This suggests that the systems under investigation should be compared in the range of $3 < \text{pH} < 10$ where the ionic strength and screening effects are moderate.

The electrolyte ions that surround the surface of the oxide, may influence the formation of charge on the particle surface through two possible mechanisms.

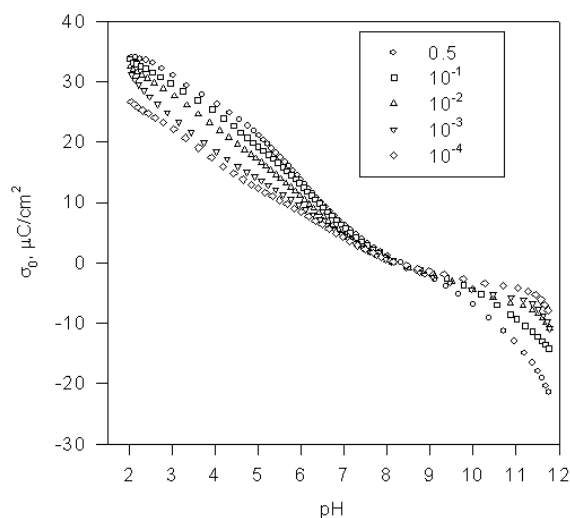


Figure 3a. σ_0 as a function of pH in aqueous CsCl of different concentrations ($0.5\text{-}10^{-4}$ M).

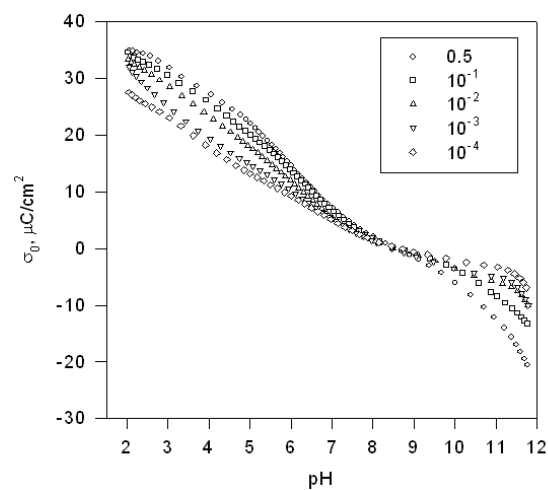


Figure 3b. σ_0 as a function of pH in aqueous of CsCl of different concentrations ($0.5\text{-}10^{-4}$ M).

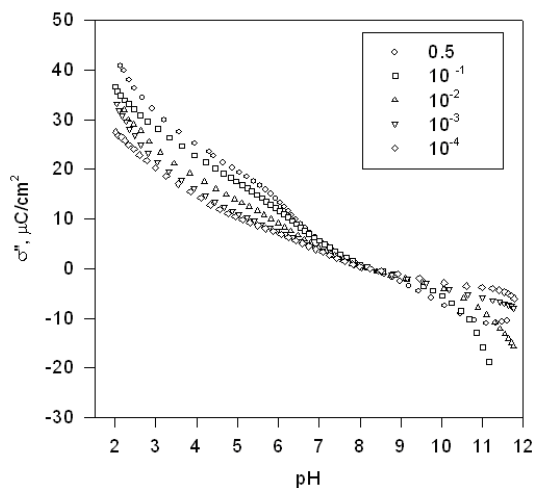


Figure 4a. σ_s as a function of pH in aqueous CsNO_3 of different concentrations ($0.5\text{-}10^{-4}$ M).

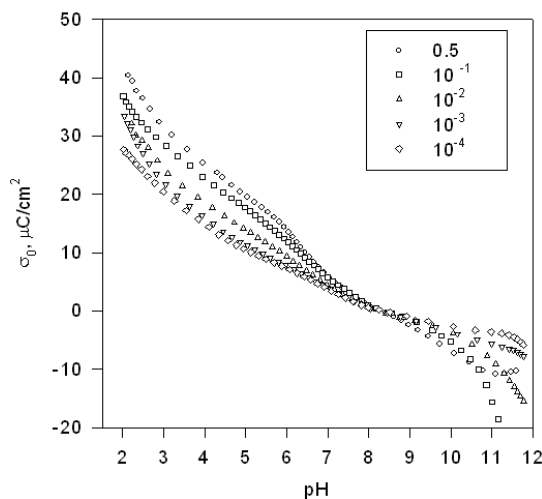


Figure 4b. σ_0 as a function of pH in aqueous CsNO_3 of different concentrations ($0.5\text{-}10^{-4}$ M).

Charge screening mechanism. In this mechanism, it is assumed that electrolyte ions play an important role of screening the charged surface. At low C_0 , the region in the locality of the particle surface is occupied by fewer amounts of ions. When a specific site on the surface takes place in surface reactions (protonation and deprotonation) it becomes charged. For the neighboring uncharged site to undergo similar surface reactions, the electrical influence of the nearby charged site has to be overcome. This makes it difficult for the site to take place in surface reactions and consequently few sites react resulting in low σ_0 . As C_0 increases, the concentration of ions around the charged surface increases. These screen the charged sites effectively such that they have no electrical influence on the neighboring uncharged sites. As a

consequence of this, uncharged sites become more susceptible to surface reactions leading to high values of σ_0 .

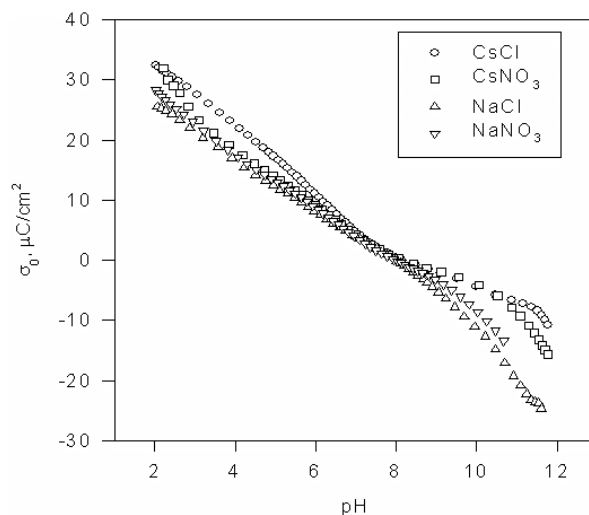


Figure 5a. σ_0 as a function of pH in various electrolytes at a concentration of 10^{-2} M.

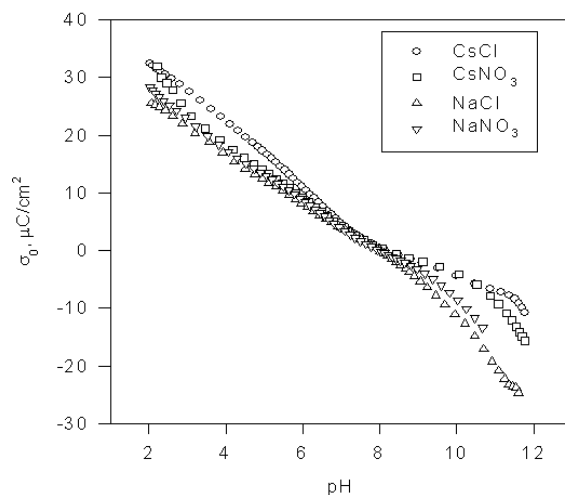
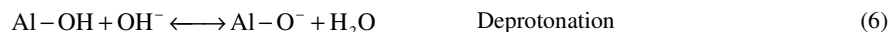


Figure 5b. σ_0 as a function of pH in various electrolytes at a concentration of 10^{-3} M.

Bond weakening mechanism. In this mechanism, it is assumed that when electrolyte ions (cations and anions) approach the particle surface, they weaken or activate the Al-OH bonds that are already on the surface. Consequently, the protonation and deprotonation reactions take place easily. At high C_0 , the Al-OH bonds on the particle surface become more activated in such a way that the thermodynamic equilibrium of the protonation and deprotonation reactions described by equations 5 and 6 shifts to the right.



Thus, higher σ_0 is developed on the surface of the particle compared with the case of low C_0 . The interaction of cations and anions with the surface hydroxyl groups may also involve binding of cations and anions at specific sites on particle surfaces. These binding reactions are considered to proceed as follows:



where Cat^+ and An^- are the respective cations and anions of the electrolyte. A schematic representation of this model is shown in Figure 6.

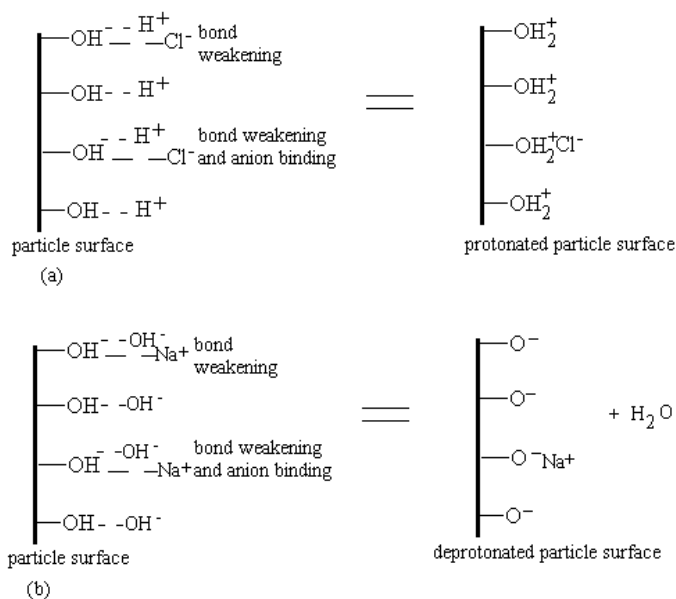


Figure 6. Schematic representation of protonation and deprotonation reactions on the particle surface, (a) protonation and (b) deprotonation.

It can be observed that in both mechanisms described above the extent of approach of cations and anions to the particle surface is limited by their hydrated sizes. Ions with small effective ion sizes can approach the surface closer than those with large sizes. It is apparent that the more close the ion gets to the surface the more it can offer charge screening or weakening of the Al-OH bonds resulting in increase in values of σ_0 . From Table 2 it can be seen that the hydrated ionic radii of Na^+ is greater than that of Cs^+ whereas Cl^- and NO_3^- ions have very close sizes of hydrated radii. This suggests that the extent of approach to the surface of Cl^- and NO_3^- ions is almost the same whereas that of cations is expected to be in the order of $\text{Cs}^+ > \text{Na}^+$.

This analysis is supported by the observations depicted in this work, for instance at a pH of 3, for $10^{-4} \leq C_0 \leq 0.5$ M, the surface charge density spans the range $18 \leq \sigma_0 \leq 30 \mu\text{C cm}^{-2}$ (Figure 1b), $18 \leq \sigma_0 \leq 28 \mu\text{C cm}^{-2}$ (Figure 2b), $22 \leq \sigma_0 \leq 32 \mu\text{C cm}^{-2}$ (Figure 3b) and $22 \leq \sigma_0 \leq$

$32 \mu\text{C cm}^{-2}$ (Figure 4b). This suggests that the binding effect of Cl^- and NO_3^- ions on positive charged sites in all systems investigated is almost the same. At the pH of 10, for $10^{-4} \leq C_0 \leq 0.5$ M, the surface charge density lies in the range of $-16 \leq \sigma_0 \leq -8 \mu\text{C cm}^{-2}$ (Figure 1b), $-10 \leq \sigma_0 \leq -5 \mu\text{C cm}^{-2}$ (Figure 2b) and $-6 \leq \sigma_0 \leq -2 \mu\text{C cm}^{-2}$ (Figure 3b and 4b). This reflects that Cs^+ ions are more effective in binding on the negative sites as compared to Na^+ ions in all systems investigated. This observation is also supported by the fact that Cs^+ ion has small hydrated ionic radius (0.33 nm) and zero hydration number, indicating that it can easily access binding sites as compared to Na^+ ion which has a hydrated ionic radius of 0.36 nm and a hydration number of 5 (Table 2).

Table 2. Ionic radii and hydration number of various ionic species [14-17].

Ion	Bare ionic radii (nm)	Hydrated ionic radii (nm)	Hydration number
H^+	-	0.28	3
OH^-	0.176	0.30	3
Na^+	0.095	0.36	5
Cs^+	0.169	0.33	0
Cl^-	0.181	0.33	1
NO_3^-	0.264	0.34	0

Comparison of experimental and literature data

After the transformation of σ'' to σ_0 , the CIP becomes the point of zero charge (PZC) these have been summarized in Table 3.

Table 3. Experimental values of CIP and σ_s of alumina obtained in this study.

Electrolyte	PZC	σ_s ($\mu\text{C}/\text{cm}^2$)
NaCl	7.8 ± 0.1	0.8 ± 0.1
NaNO_3	7.6 ± 0.2	1.4 ± 0.1
CsCl	8.5 ± 0.1	-0.9 ± 0.1
CsNO_3	8.3 ± 0.1	-0.2 ± 0.1

Table 4. PZC of α -alumina obtained from various sources.

Electrolyte	PZC	Source
NaCl	8.7-8.8	[4]
NaCl	8.4 ± 0.1	[18]
KCl, KNO_3 , KClO_4	9.1 ± 0.1	[19]
NaCl	8.8 ± 0.3	[20]
LiCl, NaCl, KCl, NaNO_3 , NaI	7.2	[21]

The PZC of alumina obtained in this study lie in the range of $7.6 \leq \text{PZC} \leq 8.5$ (Table 3) and they are within those available in literature $7.2 \leq \text{PZC} \leq 9.2$ (Table 4) for the similar material. The data presented in this work complement the available information on this oxide and they can be used for surface modelling. This is the future plan of this research and the outcome of the modelling will be reported in subsequent publications.

CONCLUSIONS

From this work following conclusions can be drawn: (1) This material exhibits a point of zero charge (PZC) in all salts investigated. The PZCs occurred at pH of 7.8 ± 0.1 , 7.6 ± 0.2 , $8.5 \pm$

0.1, 8.3 ± 0.1 for NaCl, NaNO₃, CsCl, CsNO₃ systems, respectively. (2) Below PZC, values of σ_0 increase with increase in electrolyte concentration (C_0). However above the PZC, values of σ_0 generally decrease with increase in C_0 . (3) The polarity of σ_0 can be varied through zero by varying the pH of the suspension and C_0 . (4) The ions adsorbed on the surface of the oxide play significant role on the formation of surface charge. (5) The data presented herein augment the available data of α -alumina and provide a resource for surface modelling.

ACKNOWLEDGEMENTS

The author is grateful to the Norwegian Agency for Development Cooperation (NORAD) through the Department of Chemical and Process Engineering, University of Dar es Salaam (TAN 047) for the financial support that enabled this study to be undertaken.

REFERENCES

1. Deer, W.A.; Howies, R.A.; Zussman, J. *Rock Forming Minerals*, Vol. 5 (*Non-Silicates*), 4th ed., William Clowes and Sons: London; **1965**; p 507.
2. Greenwood, N.N.; Earnshaw, A. *Chemistry of the Elements*, 2nd ed., Butterworth-Heinemann: London; **1997**; p 130.
3. Stumm, W.; Morgan, J.J. *Aquatic Chemistry, An Introduction Emphasizing Chemical Equilibria in Natural Waters*, Wiley-Interscience: New York; **1981**; p 384.
4. Cesarano, J.; Aksay, I.A.; Bleier, A. *J. Amer. Ceram. Soc.* **1988**, 71, 4.
5. Dzombak, D.A.; Morel, F.M.M. *Surface Complexation Modeling, Hydrous Ferric Oxide*, Wiley-Interscience: New York; **1990**; p 80.
6. Sverjensky, D.A.; Sahai, N. *Geochim. Cosmochim. Acta* **1996**, 60, 3.
7. Smit, W.; Holten, C.L. *J. Colloid and Interface Sci.* **1980**, 78, 1.
8. James, R.O.; Parks, G.A. in *Surface and Colloid Science*, Vol. 12, Matijevic, E. (Ed.), Plenum: New York; **1982**; p 180.
9. Hayes, K.F.; Redden, G.; Ela, W.; Leckie, J.O. *J. Colloid and Interface Sci.* **1991**, 142, 2.
10. Katz, L.E.; Hayes, K.F. *J. Colloid and Interface Sci.* **1995**, 170, 2.
11. Hunter, R.J. *Introduction to Modern Colloid Science*, Oxford University Press: New York; **1996**; pp 220-226.
12. Lyklema, J. *Fundamentals of Interface and Colloid Science*, Vol. 2, Academic Press: London; **1995**; p 284.
13. Ntalikwa, J.W.; Bryant, R.; Zunzu J.S.M. *J. Colloid Polym. Sci.* **2001**, 279, 2.
14. Lyklema, J. *Fundamentals of Interface and Colloid Science*, Vol. 1, Academic Press: London; **1991**; p 332.
15. Israelachvili, J.N. *Intermolecular and Surface Forces*, 2nd ed., Academic Press: New York; **1992**; p 172.
16. Weast, R.; Astle, M.J.; Bayer, W.H., *Hand Book of Chemistry and Physics*, 69th ed., CRC Press: New York; **1988**, p 321.
17. Adamson, A. *A Textbook of Physical Chemistry of Surfaces*, 2nd ed., Academic Press: New York; **1979**; p 158.
18. Johansen, P.G.; Buchanan, A.S. *Austr. J. Chem.* **1957**, 10, 3.
19. Yopps, J.A.; Fuerstenau, D.W. *J. Colloid Sci.* **1964**, 19, 61.
20. Ottewill, R.H.; Holloway, L.R. *Physical - Chemical Science Research Report* (National Seawater, Dahlem Workshop), **1975**; pp. 599 - 621.
21. Todorovic, Z.; Milonjic, S. *J. Serb. Chem. Soc.* **2004**, 69, 1063.